Available online at www.sciencedirect.com
ScienceDirect
Chemical Geology 245 (2007) 285–304
CHEMICAL GEOLOGY INCLUDING ISOTOPE GEOSCIENCE
www.elsevier.com/locate/chemgeo

Clinoptilolite as a new proxy of enhanced biogenic silica productivity in lower Miocene carbonate sediments of the Bahamas platform: Isotopic and thermodynamic evidence

Anne Marie Karpoff [a,*], Christine Destrigneville [b], Peter Stille [a]

[a] EOST – Centre de Géochimie de la Surface, CNRS-UMR 7517, 1 rue Blessig, 67084 Strasbourg, France
[b] Laboratoire des Mécanismes de Transfert en Géologie – Université de Toulouse, CNRS-IRD-OMP-UMR 5563, 14 avenue E. Belin, 31400 Toulouse, France

Received 6 October 2006; received in revised form 15 August 2007; accepted 30 August 2007

Editor: B. Bourdon

Abstract

Massive clinoptilolite authigenesis was observed at about 1105 meters below sea floor (mbsf) in lower Miocene well-compacted carbonate periplatform sediments from the Great Bahama Bank [Ocean Drilling Program, ODP Leg 166, Site 1007]. The diagenetic assemblage comprises abundant zeolite crystallized within foraminifer tests and sedimentary matrix, as well as Mg smectites. In carbonate-rich deposits, the formation of the zeolite requires a supply of silica. Thus, the objective of the study is to determine the origin of the silica supply, its diagenetic evolution, and consequently the related implications on interpretation of the sedimentary record, in terms of local or global paleoceanographic change. For lack of evidence for any volcaniclastic input or traces of Si-enriched deep fluids circulation, an *in situ* biogenic source of silica is validated by isotopic data and chemical modeling for the formation of such secondary minerals in shallow-water carbonate sequences. Geochemical and strontium isotopic data clearly establish the marine signature of the diagenetic zeolite, as well as its contemporaneous formation with the carbonate deposition (Sr model ages of 19.6–23.2 Ma). The test of saturation for the pore fluids specifies the equilibrium state of the present mineralogical assemblage. Seawater–rock modeling specifies that clinoptilolite precipitates from the dissolution of biogenic silica, which reacts with clay minerals. The amount of silica (opal-A) involved in the reaction has to be significant enough, at least 10 wt.%, to account for the observed content of clinoptilolite occurring at the most zeolite-rich level. Modeling also shows that the observed amount of clinoptilolite (~19%) reflects an *in situ* and short-term reaction due to the high reactivity of primary biogenic silica (opal-A) until its complete depletion.

The episodic occurrence of these well-lithified zeolite-rich levels is consistent with the occurrence of seismic reflectors, particularly the P2 seismic sequence boundary located at 1115 mbsf depth and dated as 23.2 Ma. The age range of most zeolitic sedimentary levels (biostratigraphic ages of 21.5–22 Ma) correlates well with that of the early Miocene glaciation Mi-1 and Mi-1a global events. Thus, the clinoptilolite occurrence in the shallow carbonate platform environment far from

* Corresponding author. Postal address: EOST – Centre de Géochimie de la Surface, 1 rue Blessig, 67084 Strasbourg-Cedex, France. Tel.: +33 390 240426; fax: +33 390 240402.
E-mail addresses: amk@illite.u-strasbg.fr (A.M. Karpoff), cdestri@lmtg.obs-mip.fr (C. Destrigneville), pstille@illite.u-strasbg.fr (P. Stille).

0009-2541/$ - see front matter
doi:10.1016/j.chemgeo.2007.08.011

volcanogenic supply, or in other sensitive marine areas, is potentially a significant new proxy for paleoproductivity and oceanic global events, such as the *Miocene events*, which are usually recognized in deep-sea pelagic sediments and high latitude deposits.

Keywords: Zeolite; Smectite; Biogenic silica; Modeling; Sr isotopes; Productivity; Miocene; Mi-event; Bahamas carbonate platform; Ocean Drilling Program Leg 166; Site 1007

1. Introduction

Among other oceanic tectonic and sedimentary settings, the carbonate platform and margin sequences are ideal archives, particularly for their structures and types of deposits, to study global changes in sea-level (among others: Haq et al., 1987; Anselmetti et al., 2000; Betzler et al., 2000; Reijmer et al., 2002), and for paleoceanographic variations, paleoproductivity and environmental studies (*i.e.* Eberli, 1991; Roof et al., 1991; McKenzie et al., 1993; Eberli et al., 1997; Camoin and Dullo, 1999; Swart and Eberli, 2005). Integrated studies on such marine environments usually provide more information on the carbonate system (production, biofacies…) *per se* than on the silica transfer and cycle fluctuations.

As suggested by previous studies on drilled carbonate platforms (McKenzie et al., 1993; Winterer et al., 1995; Swart et al., 2000), active and various-scale circulation of fluids occurs in the upper portion of the strata, as well as in deeper levels (Kramer et al., 2000; Caspard et al., 2004). Fluids flow is primarily recognized by early recrystallization of carbonates in the subsurface and by geochemical trends (Elderfield et al., 1993; Henderson et al., 1999; Swart, 2000; Frank and Bernet, 2000; Malone et al., 2001; Melim et al., 2002; Reuning et al., 2002). Fluid circulation enhances inorganic chemical reactions, and in concert with microbial activity, controls the diagenetic carbonate modifications, as well as the rock porosity and permeability along localized flows conduits. Hence, the diagenetic transformations could modify significantly the seismic sequence boundaries and signals, and consequently the sea-level reconstructions and productivity records. Moreover the water–rock interactions within sediments, particularly within margins and shallow-water deposits, represent important mechanisms in the chemical transfer between lithosphere and hydrosphere.

On the western flank of the Great Bahama Bank (GBB), at Site 1007 drilled during ODP Leg 166 at the toe-of-slope of the periplatform, the lower Miocene sedimentary section is distinguished from the overlying units by a specific authigenic paragenesis comprising Mg smectite and abundant Na–K-clinoptilolite filling foraminifers and pore spaces. This diagenetic silicate paragenesis is not usually found in shallow-marine and almost pure carbonate sediments. The intense diagenetic transformation, which affects the physical properties of deposits, is recorded by sediment mineralogical and geochemical compositions as well as the interstitial fluid chemistry trends. Such a process implies either the remobilization of a Si-rich component (mineral phase, fluid) promoted by *in situ* water–rock reactions, or the incursion of a deep fluid linked to particular geodynamical and/or tectonic event; both assumptions were first considered by Karpoff et al. (2001, 2002).

Hence, the origin of the excess of silica necessary for the formation of clay–zeolite assemblage has to be ascertained: does it result from a non-preserved biogenic phase, or a lithic contribution or a fluid incursion? The first goal of this study is to specify the conditions of formation of the secondary smectite–clinoptilolite paragenesis, and then, as a result of this approach, the origin and type of reactive silica involved in the process is clearly established. Thus, the timing for the initiation of the specific diagenetic evolution in such shallow sequences is identified. Our Sr-isotopic data allows us to determine the age and to point out the origin of the sedimentary components (among marine, detrital, crustal, or diagenetic origins). Modeling validates the hypothesis of *in situ* syndepositional water–rock interactions, and helps define the mineralogical terms, particularly biogenic opal, and the fluid chemistries involved in the processes. Accordingly, the paleoceanographic implications and paleoproductivity records are linked to these objectives and results, particularly the potential relationship between the described processes and the coeval early Miocene climatic changes recorded in hemipelagic and deep-sea realms (*i.e.* Mutti et al., 1997; Paul et al., 2000; Zachos et al., 2001a,b; John et al., 2003; Anderson and Delaney, 2005).

2. Background

2.1. Geological setting: the Bahamas Transect

The western flank of the Great Bahama Bank (GBB) consists of a series of prograding sedimentary sequences produced by large-scale sea-level fluctuations from late Oligocene to Holocene in a tectonically stable system

(Eberli et al., 1997). The objectives of the "Bahamas Transect" of ODP Leg 166 were first to document the glacio-eustatic changes recorded in the sequences over the past 25 my, and second to ascertain a potential fluid flow and its diagenetic fingerprint. Five drilled sites (Sites 1003 to 1007) recovered Neogene carbonate sediments primarily composed of material from various sources: platform-derived, pelagically derived, and detrital. The latter are hypothesized to originate from southern areas, for instance Cuba and Hispaniola islands. Pelagic and siliciclastic materials become more important during sea-level lowstands. The Sites 1005, 1004 and 1003 closest to the margin (Fig. 1), were more influenced by carbonate production on the platform top showing high rates of accumulation during sea-level highstands and reduced or little sedimentation during lowstands. Deposition rates were slightly reduced at the most distal Sites 1006 and 1007, in the upper 50 to 100 meters below seafloor (mbsf). The deepest drilled site, Hole 1007C (Figs. 1 and 2), in about 647 m of water depth, penetrated upper Oligocene sediments at 1235.4 mbsf. The nearly complete 900-m-thick Miocene section consists of a succession of bioturbated, periplatform limestone with interbeds of turbiditic packstone, grainstone, and floatstone. Details of the sedimentology and rates of deposition are provided by Eberli et al. (1997), Shipboard Scientific Party (1997), Betzler et al. (1999). At depths below 1100 mbsf, an increase in overall compaction and lithification features is observed. Several studies described the platform architecture features and carbonate diagenesis records, such as lithification and dolomitization processes (references in *Marine Geology*, 2002, sp. vol. 185). In the sequences at shallow sites, dolomitization linked to a present-day geothermal large-scale convection was modeled (Caspard et al., 2004). Nevertheless, Kramer et al. (2000) conclude that the pore fluid profiles in the lower Pliocene–Miocene sequences are dominated by diffusion and do not show significant evidence of subsurface advective flow. Thus, deeper interstitial waters are believed to be *in situ* fluids that have evolved mainly through interactions with the sediments.

The siliciclastic fraction in the Miocene carbonate deposits from Site 1007, as well as Pliocene sequences from more distal Site 1006, were first studied by Karpoff et al. (2002) specifically for determining its variations in relation to changes in source, climatic and environmental conditions through time.

2.2. Mineralogy and geochemistry of lower Miocene deposits

The mineralogical and geochemical data were previously detailed by Karpoff et al. (2002). Mineralogical compositions were obtained from X-ray diffraction analyses (XRD) of non-oriented powders of bulk sediments (sampling in clay-rich layers and poorest carbonate layers) and from 4 types of oriented aggregates of the extracted carbonate-free <2 μm fractions (clay fractions). Bulk samples were observed under scanning electron microscope (SEM) and fine fractions under transmission electron microscope (TEM, STEM), both equipped with an energy dispersive X-ray analyser (EDS) allowing chemical analyses of the specific authigenic minerals. Major and trace element concentrations in bulk samples are measured by ICP-AES (ARL® 3500 C) and ICP-MS (VG® Plasmaquad PQ2+) following the procedure described by Samuel et al. (1985). Major elements are expressed in percentage of oxides, the weight loss of ignition (LOI) in percentage, and trace elements in ppm, for 100 g of dried sample. Relative precision is of ±10% for the ICP-AES data and ±5% for the ICP-MS data, on the 1 sigma level. The interstitial waters were routinely analyzed on board, from squeezed cakes of 5 to 15 cm long whole sections (Shipboard Scientific Party, 1997). Data are reported in Tables 1 and 2.

In the Miocene carbonate deposits (seismic sequences *h* to *q*; Fig. 1), the mineralogical composition of clay-rich intervals appears relatively uniform for the prevalent phases and non-carbonate fraction. Nevertheless, the occurrence of authigenic phases characterizes the middle and lower Miocene deposits, and the sequences *k* to *n* differ from the younger ones by a low detrital clay input (scarce illite) but prevalent well-crystallized smectites. The diagenetic character of the smectites (morphology, lower crystallinity) slightly increases with depth. In the lower Miocene deposits (910–1216 mbsf, sequences *o* to topmost *r*) a major mineralogical change occurs in an interval at ~1100 mbsf with the development, together with authigenic smectite, of abundant clinoptilolite and celestine (Figs. 2 and 3). Within this interval a distinct thin zeolite-free clay layer was sampled at 1104.54 mbsf. The biostratigraphic age of the studied interval is ~21.5 Ma (top of foraminifer Zone N4 and nannofossil Zone NN2/1 boundary; Eberli et al., 1997). In this level of recorded lowered sedimentation rate (<2 cm ky^{-1}), the clayey interval from the wackestone facies contains at least 40% of non-carbonate phases (<60% $CaCO_3$ estimated from bulk-rock analyses, *in* Karpoff et al., 2002). The main chemical tracer of the clinoptilolite interval appears to be the high barium content increasing to 750 ppm in bulk rock (<80 ppm in the overlying zeolite-free sequences). Below the lower Miocene deposits, the decrease in strontium contents reflects carbonate recrystallization. The dark-colored intervals of

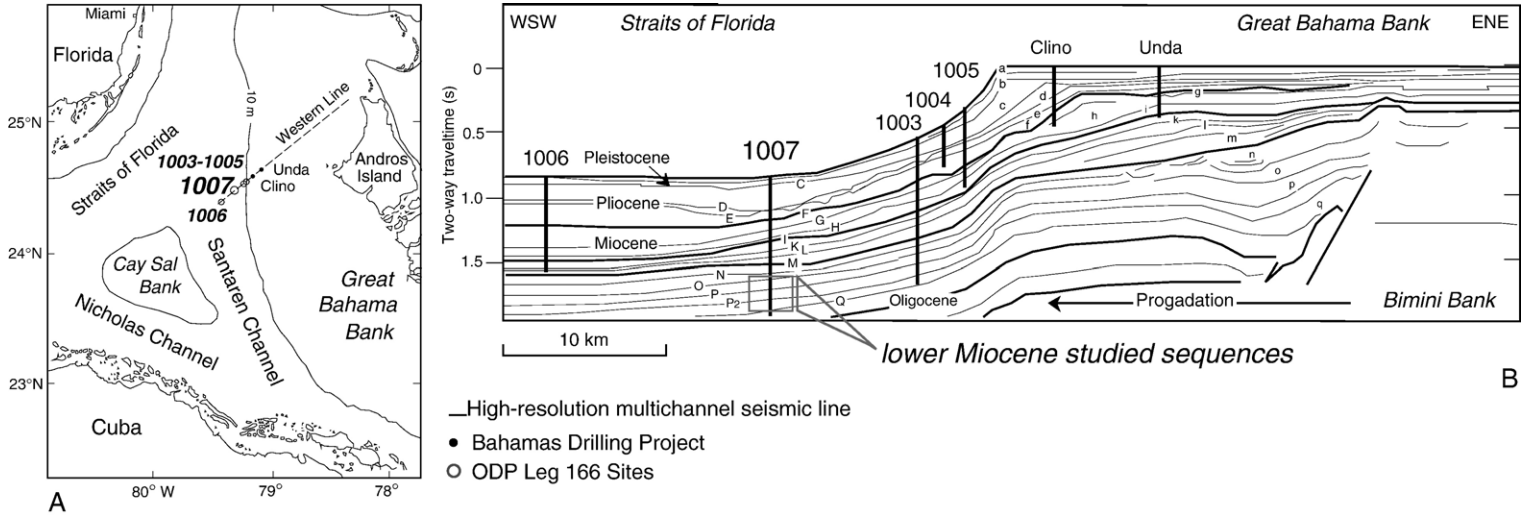

Fig. 1. A. Location map of the ODP Leg 166 Bahamas Transect along the extension of the "Western Geophysical Seismic Line" into the Straits of Florida. B. Geometry of the GBB western margin and position of the drilling sites; (a,...) seismic sequences and (A,...) seismic boundaries (from Eberli et al., 1997).

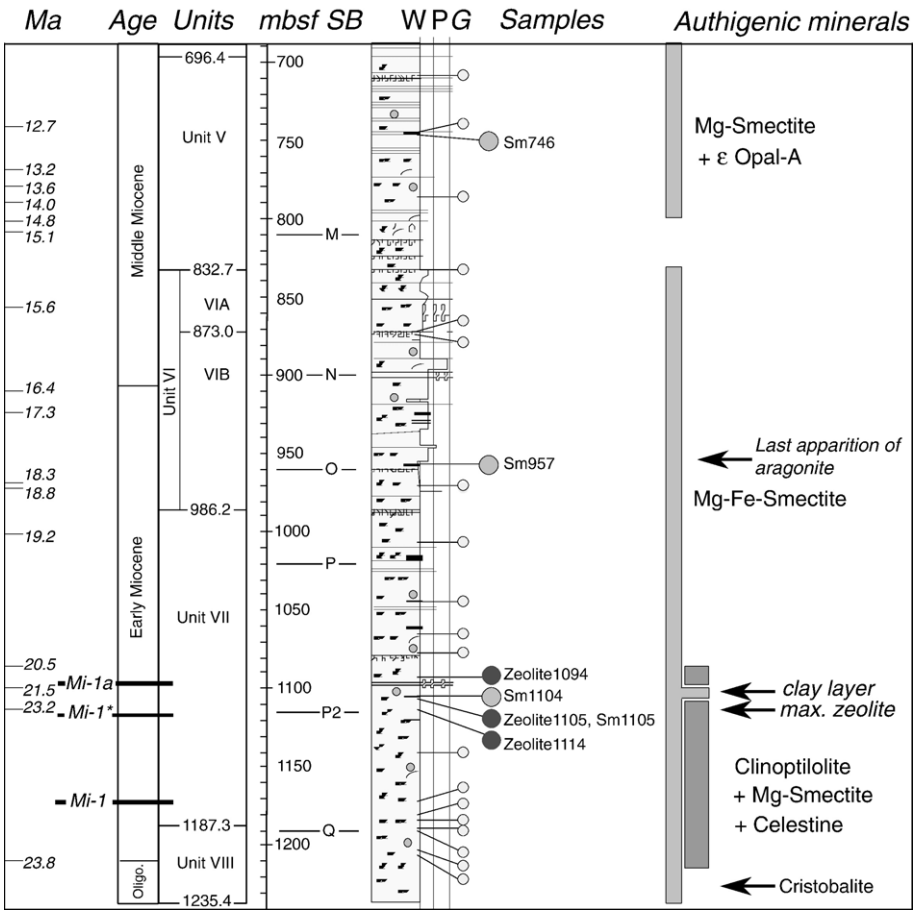

Fig. 2. Simplified lowermost lithostratigraphic core at Site 1007. Facies (W: wackestone, P: packstone, G: grainstone), seismic boundaries (SB: M to Q), and ages (Ma) from biostratigraphic data from Shipboard Scientific Party (1997). mbsf: meters below seafloor. The locations of Miocene events (from Miller et al., 1991; Mi-1* from Paul et al., 2000) are calculated extrapolating sedimentation rates. Location of samples (large spots) and their relative names used in this study (small grey points: other samples described *in* Karpoff et al., 2002).

the lower Miocene strata also contain a substantial total organic carbon content (~1% TOC; Kramer et al., 2000). In the sediments neither volcanic fragments nor glass shards were found or described in adjacent sites. The occurrence of the diagenetic silicate paragenesis (zeolite+smectite) is associated with an increase in compaction–dissolution features, and correlates with the position of the seismic sequence boundary P2 (at 1115 mbsf; Eberli et al., 1997). The transition to the upper Oligocene sequence (boundary at 1216 mbsf) is marked by the occurrence of black chert nodules.

The present study is focused on the zeolitic samples (Fig. 2). Clinoptilolite occurs chiefly in the structurally well-preserved often recrystallized foraminifera tests and in pore spaces of the matrix of the wackestone level. The crystals of clinoptilolite within the most zeolitic samples (*i.e.*, interval 1094–1114 mbsf) are generally well formed and large sized, from few microns up to 20 μm (Fig. 3, and *in* Karpoff et al., 2002).

3. Methodology

3.1. Strontium isotope analyses

The samples for isotopic analyses were selected for their high contents in authigenic phases (from XRD, SEM and chemical data): the smectite-rich zeolite-free sample at 1104.54 mbsf and three zeolite-rich samples at 1093.66, 1104.75, and 1114.22 mbsf; the sample at 1104.75 mbsf is the clinoptilolite richest sample. These four samples were reported in the following as Sm1104, Zeolite1094, Zeolite1105 and Zeolite1114, respectively with index -R for insoluble residue and -L for the equivalent leachate (Table 3). In order to obtain isotopic

Table 1
Compositions of interstitial fluids from Site 1007 sediments (Shipboard Scientific Party, 1997)

Sample [a]	Depth	pH	Alk	Sal	Cl^-	Na^+	Mg^{2+}	Ca^{2+}	SO_4^{2-}	H_4SiO_4	K^+	Sr^{2+}	Fe^{2+}	NH_4^+
	mbsf		mM	g/kg	mM	mM	mM	mM	mM	μM	mM	μM	μM	μM
1007B-1H-4, 140-150	5.90	7.61	2.87	35.5	562	475	53.6	10.9	28.2	50	10.3	129	5.6	47
1007B-8H-4, 135-150	72.85	8.08	20.47	42.5	689	585	57.1	10.0	20.9	286	11.9	968	27.9	2390
1007B-18X-2, 0-15	158.30	8.05	22.88	49.5	803	689	63.0	12.0	23.1	297	14.3	898	12.5	3188
1007B-32X-1, 135-150	287.35	7.82	11.75	55.0	905	738	59.4	23.9	28.4	318	15.8	723	19.2	2159
1007C-17R-6, 99-114	463.33	7.65	9.80	56.0	932	769	54.8	22.9	22.2	403	16.5	935	22.5	3524
1007C-28R-3, 103-116	565.32	7.65	10.79	53.0	961	779	33.6	14.8	5.7	779	16.5	3237	20.0	7031
1007C-37R-1, 0-12	648.30	7.11	14.74	52.0	899	754	27.9	12.1	2.2	775	15.8	3504	18.8	7472
1007C-47R-2, 0-14	745.70	7.28	10.94	54.0	945	803	28.7	14.1	1.3	725	17.6	3802	*20*	9068
1007C-57R-2, 0-10	842.12	7.11	15.35	54.5	955	820	31.4	15.0	1.7	729	16.9	4095	*20*	11131
1007C-66R-2, 28-39	928.98	7.04	11.48	56.5	1001	827	27.6	15.5	0.7	*730*	14.3	4780	*20*	12491
1007C-72R-2, 0-5	986.41	*7.00*	*7.50*	55.5	971	820	27.6	15.1	1.8	*730*	12.9	4300	*20*	10281
1007C-75R-1, 50-60	1014.40	*7.00*	*7.50*	*55.0*	809	688	22.3	14.2	3.5	*730*	10.0	3740	*20*	6592

Italic values are fixed from values measured in preceding levels and trend (see text).
[a] ODP convention sample notation: Site, core, section, interval (cm); mbsf: meters below seafloor; Alk: alkalinity; Sal: salinity.

data on the sole zeolite, several acid treatments were done on bulk-rock fragments. The samples were sequentially extracted in 3 steps with 0.01 N acetic acid (HAc), 0.1 N HCl and 1 N HCl. The extractions were conducted in centrifuge tubes (polypropylene, 15 ml). After the third step the residues were completely dissolved in a HF–HNO_3 mixture and likewise analyzed by ICP-MS and ICP-AES (Table 4). For more detail see Steinmann and Stille (1997).

The control of the effect of the sequential acid treatments on the carbonates and authigenic silicates was made by observation of the residues under SEM. The two first steps preserved parts of the carbonates in the residues, but the final step with 1 N HCl allows dissolving the carbonates without any noticeable damage on the authigenic zeolite (Fig. 4). A small part of residual carbonate could be trapped within zeolite crystals and few celestine, which is cogenetic with zeolite, and not fully dissolved. Thus, the isotopic data obtained on these residues and corresponding leachates should be the isotopic signatures of the authigenic phases and the associated carbonates, respectively.

Standard techniques were applied for Sr-isotope analysis. Sr enrichment and separation from the bulk sample used cation exchange resin with ammonium citrate and 1.5 N, 4 N, and 6 N HCl as eluents. The analyses were performed on a fully automatic VG Sector® thermal ionization mass spectrometer (TIMS) with a 5-cup multicollector. Sr was loaded with nitric acid on a W single filament using Ta_2O_5 as an activator. The ratio $^{86}Sr/^{88}Sr = 0.1194$ was used for fractionation correction. During the measuring period the NBS 987 Sr standard yielded $^{87}Sr/^{86}Sr = 0.710258 \pm 0.000013$ (±standard deviation, $n = 9$).

The Sr-isotope results are reported in Table 3 and Fig. 5. The Sr-isotopic ages were assigned from the

Table 2
Chemical compositions in oxide wt.% of two bulk rocks (BR) from lower Miocene sediments at Site 1007 and their respective constituting smectites (Sm) and zeolite (Zeolite)

Sample	SiO_2	Al_2O_3	MgO	CaO	Fe_2O_3	TiO_2	Na_2O	K_2O	LOI
1007C-47R-2, 41–42, 746.11 mbsf									
BR746	35.1	12.10	2.33	24.22	1.4	0.21	2.06	0.37	22.26
Sm746	66.01	22.41	6.64	0	0	0	0	0	4.94
1007C-84R-4, 10–14, 1104.75 mbsf									
BR1105	18.0	3.75	0.98	36.89	4.93	0.15	0.93	0.51	26.53
Sm1105	62.24	17.87	6.06	0	6.73	0	0	2.36	4.75
Zeolite1105	63.52	12.64	0	1.95	0	0	4.18	2.05	15.62

LOI: % Loss on ignition 1000 °C (mineral water loss, CO_2…).
BR data from ICP-AES analyses.
Sm and zeolite data from STEM–EDX analyses on selected particles (average of $n > 8$ analyses).

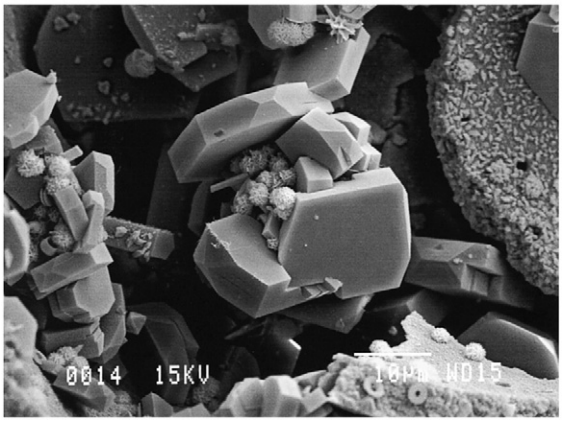

Fig. 3. SEM microphotograph of clinoptilolite crystals filling foraminifera tests in bulk calcareous packstone. Small opal lepispheres occur between crystals. Untreated bulk sample 1007C-84R-4, 10–14 from 1104.75 mbsf level (BR1105).

seawater curve established by Hodell et al. (1991). The biostratigraphic ages were estimated from shipboard and shore-based refined markers (Shipboard Scientific Party, 1997).

3.2. Thermodynamic Modeling Procedure

3.2.1. Computer code

Calculations were carried out with the KINDIS computer code (Madé et al., 1990). In the static option, KINDIS calculates the chemical speciation of a fluid from its major elements total concentrations and gives its saturation state (SI: saturation index) regarding to chosen minerals. In the dynamic option, KINDIS calculates the chemical evolution of the fluid and of the minerals during a water–rock interaction process in a closed system. The chemical constituents of the altered rock are progressively added to 1 kg of fluid. The program characterizes the secondary minerals assemblage and the fluid chemistry, which are in thermodynamic equilibrium at each step of the alteration. No kinetic laws of dissolution or precipitation are introduced in the program, but the water/rock ratio (W/R) gives an estimate of the degree of alteration: a high W/R value corresponds either to a fluid-dominated alteration or to the early stage of the alteration process, and a low W/R ratio corresponds to a high degree of alteration in which the limiting case is fluid exhaustion. Thermodynamic data for the fluid and the minerals in the KINDIS database, and especially for opaline silica (opal-A), are from Helgeson et al. (1978).

Three steps were followed in this study. The first step consisted in testing the chemical stability of the present-day deposit composed of the observed mineralogical phases and of the interstitial fluids. The second step was to predict the evolution of the secondary mineral assemblage when seawater–rock interaction occurs in one of the biogenic opal-enriched levels and to test the assumption that the occurrence of clinoptilolite in the altered rock is related to an initial opaline silica content. In the third step, a mass balance calculation was carried out on the clinoptilolite-rich horizon in order to evaluate the initial opal content in that layer, and to compare the results of the modeling with the observations.

3.2.2. Components and modeling conditions

Concerning the first step of the modeling, the saturation state of twelve interstitial fluids sampled from 5.9 mbsf to 1014.4 mbsf along the Site 1007 profile was calculated with respect to carbonates, smectites and zeolites. The compositions (total elementary concentrations) of the fluids are given in Table 1. As the pH, alkalinity and SiO_2 molarity values were lacking in the shipboard pore fluid data for the lowermost fluids sampled at 986.41 and 1014.4 mbsf, thus we attributed to both samples a pH value and a SiO_2 molarity close to that measured over the previous 100 m and in the range

Table 3
Sr-isotope compositions of the sample-leachates (-L: 3 steps, soluble carbonate fractions) and the sample-residues (-R) of lower Miocene samples from ODP Site 1007

Samples	Steps	$^{87}Sr/^{86}Sr$	2σ mean	Model Age[a]
				Ma (±)
Leachates				
Zeolite1094-L	HAc (0.01 N)	0.708401	0.000011	21.7 (0.2)
	HCl (0.1 N)	0.708385	0.000011	21.9 (0.2)
	HCl (1 N)	0.708381	0.000014	22.0 (0.3)
Sm1104-L	HAc (0.01 N)	0.708364	0.000015	22.3 (0.3)
	HCl (0.1 N)	0.708367	0.000014	22.2 (0.3)
	HCl (1 N)	0.708397	0.000013	21.7 (0.2)
Zeolite1105-L	HAc (0.01 N)	0.708376	0.000013	22.1 (0.2)
	HCl (0.1 N)	0.708371	0.000011	22.1 (0.2)
	HCl (1 N)	0.708338	0.000013	22.7 (0.2)
Zeolite1114-L	HAc (0.01 N)	0.708371	0.000013	22.1 (0.2)
	HCl (0.1 N)	0.708352	0.000015	22.5 (0.3)
	HCl (1 N)	0.708313	0.000014	23.1 (0.3)
Residues				
Zeolite1094-R		0.708523	0.000074	19.6 (1.3)
Sm1104-R		0.707722	0.000016	50[b]
Zeolite1105-R		0.708473	0.000047	20.5 (0.8)
Zeolite1114-R		0.708306	0.000013	23.2 (0.2)

SRM 987 (this study) = 0.710250; SRM 987 (Hodell et al., 1991) = 0.710235.
[a] Model ages according to Hodell et al. (1991), after standard adoption.
[b] Age deduced from DePaolo and Ingram (1985).

Table 4
Chemical composition (trace elements in ppm) of the sample-residues (-R, non-carbonate fractions) from lower Miocene deposits, Site 1007

Sample	Zeolite1094-R	Sm1104-R	Zeolite1105-R	Zeolite1114-R
mbsf	1093.66	1104.54	1104.75	1114.22
Sr	1191.5	818.9	1053.3	1235.2
Ba	17.5	70.7	185.6	609.4
V	20.5	55.2	30.9	47.0
Ni	40.9	70.7	58.4	81.8
Cr	68.7	87.7	67.0	112.5
Zn	38.0	87.7	49.8	75.7
Cu	8.8	25.5	15.5	20.4
Sc	1.0	5.2	3.9	5.7
Y	3.7	9.6	9.8	10.8
Zr	0.0	2.8	6.9	12.3
La	4.27	7.91	8.95	9.49
Ce	4.25	16.44	8.69	10.37
Pr	0.95	2.83	1.92	2.19
Nd	4.13	12.07	7.85	8.96
Sm	0.82	2.98	1.68	1.92
Eu	0.19	0.34	0.41	0.63
Gd	0.69	2.16	1.51	2.0
Tb	0.12	0.38	0.24	0.35
Dy	0.76	2.53	1.68	2.0
Ho	0.16	0.50	0.38	0.47
Er	0.39	1.24	1.01	1.06
Tm	0.06	0.20	0.14	0.22
Yb	0.31	1.19	0.82	0.92
Lu	0.04	0.16	0.14	0.18

of the observed trends. The value for alkalinity was fixed at 7.5 mM in order to induce a slight under-saturation of the lowermost fluids towards aragonite, according to the observed disappearance of aragonite below 950 mbsf. This has no influence on the saturation state of the non-carbonate minerals.

In order to test the index of saturation of the smectites and clinoptilolites whose chemical compositions have been analyzed (data from stem measurements on several defined particles), three smectites were chosen at the respective depths of 746.11 mbsf, 957.54 mbsf and 1104.75 mbsf, as well as the zeolite located at 1104.75 mbsf (Fig. 2, Table 2). In the following, they are respectively called Sm746, Sm957, Sm1105 and Zeolite1105. Sm746 was described in Karpoff et al. (2002) as the prevalent smectite representative of the middle Miocene lithologic unit V, where carbonate recrystallization is weak and where no authigenic zeolite was found. Sm957 is the smectite of the first sample from the level where aragonite disappears. Sm1105 and Zeolite1105 are the coexisting smectite and clinoptilolite in the zeolite-rich sample. Their thermodynamic constants were calculated at 25 °C using the Chermak and Rimstidt's method (1989) and introduced in the KINDIS database (see Table 5 for their respective structural formulae and associated log(K)). Calculations were carried out as well for the common phyllosilicates and carbonates whose thermodynamic data are already included in the KINDIS database (Table 5). Only those which are interesting for our purpose, or which will occur in the further water–rock interaction modeling are presented. The temperature was set at the constant value of 25 °C over the entire profile for the following two reasons: (1) 25 °C corresponds to the given temperature of the method used for the calculation of log(K); (2) the *in situ* bottom hole temperature in Site 1007 was only measured through 250 mbsf and varies from top to bottom from 6 °C to 18 °C (Shipboard Scientific Party, 1997; Nagihara and Wang, 2000). Using 25 °C instead of the measured values will lead to an under-estimate and over-estimate in the saturation state of the fluids with respect to the carbonates and to the phyllosilicates and zeolites, respectively. This effect will become negligible below 500 mbsf, where the estimated temperature should be around 20 °C.

In the second step of the modeling, where predicting the evolution of the seawater alteration of an opal-enriched level is of interest, the chemical composition of the bulk-rock sample at 746.11 mbsf (BR746) was chosen (Table 2). This sample is a clay-rich horizon where Sm746 is the prevalent clay mineral, and where an excess of silica in the chemical analyses (STEM) presumes a contamination by opaline silica (Karpoff et al., 2002). Given that opal could be preserved in spite of its high reactivity in the first 20 cm of a deposit (Van Cappellen, 1996), the sample BR746 was considered to have not undergone silica diagenesis, and being primary sediment before any further seawater alteration. Modeling its alteration will test the assumption that

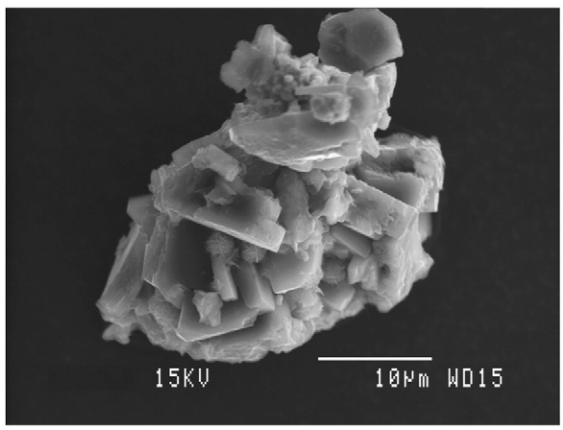

Fig. 4. SEM microphotograph of the analyzed residue after HCl-1 N leaching of the bulk rock: the calcitic matrix and tests are dissolved and the fraction is only composed of clinoptilolite crystals as aggregates and foraminifera molds. Sample 1007C-84R-4, 10–14 from 1104.75 mbsf level (Zeolite1105-R).

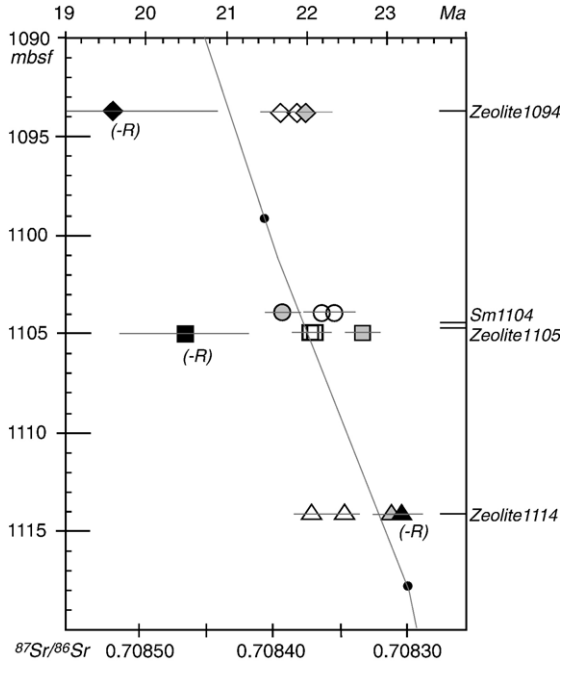

Fig. 5. Sr-isotopic ages (Ma) of samples from 1090 to 1115 mbsf interval at ODP Site 1007. White symbols stand for HAc and HCl-0.1 N sample-Leachates data, and grey symbols for HCl-1 N sample-Leachates (total soluble carbonate fractions) data. Black symbols stand for samples-Residues (zeolites). Sedimentation rate line and small black points refer to the available biostratigraphic ages from Eberli et al. (1997).

clinoptilolite can precipitate when the chemical elements of an opal- and clay-enriched rock are simply remobilized. Then, tests with different contents of opaline silica in BR746 were carried out considering the two other following cases: BR746 without any opaline silica, and BR746 with 6 wt.% extra opaline silica. Seawater–rock interactions were carried out at 25 °C, as well as in the first step of modeling.

4. Rr-isotopic characterization of authigenic clay and zeolite

In oceanic sediments, the Sr-isotopic ratio of primary and secondary minerals is used to discriminate between their different origins, as it records the signal of the source of the mineral components: marine, detrital, diagenetic, crustal, or hydrothermal. The Sr-isotope ratio of the authigenic minerals corresponds to that of the fluid from which they form, at the site of precipitation. The $^{87}Sr/^{86}Sr$-isotopic composition of pore fluid could have been modified, in comparison to that of contemporaneous seawater, either by less-radiogenic oceanic crust and/or hydrothermal input or by more radiogenic Sr derived from the alteration of terrigenous material or meteoric water, or could have been evolved through time by carbonate dissolution–recrystallization (references in Elderfield et al., 1993; Banner, 1995). Strontium isotope ratios have also proven to be a useful indicator of water–rock interaction. Then, strontium isotopic analyses have been performed in order to ascertain the origin of the authigenic clinoptilolite and above all to establish the source of silica involved in the diagenetic process in the GBB lower Miocene carbonates. The marine biogenic carbonate retains the isotopic composition of seawater at the time of formation (references in Hodell et al., 1991). The authigenic minerals also use dissolved species and form in isotopic equilibrium with contemporaneous seawater or interstitial fluid. To a close approximation the very small amount of marine dissolved Rb^+ scavenged by zeolite and that could go along with K did not have significant impact

Table 5
Structural formulae and thermodynamic constants (log(*K*) at 25 °C) of the smectites and zeolites used in the modeling

Mineral	Depth (mbsf)	Structural formulae	log(*K*)
Site 1007 analyzed smectites			
Sm746	746.11	$Si_4Al_{1.6}Mg_{0.6}O_{10}(OH)_2$	−33.81
Sm957	957.54	$Si_4Al_{1.5}Fe_{0.15}Mg_{0.48}Ca_{0.12}O_{10}(OH)_2$	−30.10
Sm1105	1104.75	$Si_{3.93}Al_{1.33}Fe_{0.32}Mg_{0.57}K_{0.19}O_{10}(OH)_2$	−30.41
Site 1007 analyzed clinoptilolite			
Zeolite1105	1104.75	$Si_{4.86}Al_{1.14}Ca_{0.16}Na_{0.62}K_{0.2}O_{12}\cdot 4H_2O$	−31.60
KINDIS database phyllosilicates and zeolites			
Kaolinite		$Si_2Al_2O_5(OH)_4$	−39.14
Na-montmorillonite		$Si_{3.667}Al_{2.333}Na_{0.333}O_{10}(OH)_2$	−47.95
Mg-montmorillonite		$Si_{3.667}Al_{2.333}Mg_{0.1665}O_{10}(OH)_2$	−48.20
K-clinoptilolite		$Si_{10}Al_2Ca_{0.1}K_{1.8}O_{28}\cdot 8(H_2O)$	−66.99

log(*K*) for *in situ* analyzed minerals calculated following Chermak and Rimstidt (1989).
log(*K*) for KINDIS database minerals from Helgeson et al. (1978).

on the $^{87}Sr/^{86}Sr$-isotopic value of the authigenic Sr-rich clinoptilolite. Moreover, at nearby Site 1006, the interstitial fluid shows divergent trends in Rb^+ and K^+ concentrations and the slight increase of Rb^+ concentration downhole is interpreted as a clayey detrital matter contribution by ion exchange (De Carlo and Kramer, 2000).

4.1. Isotopic results on the carbonate sediments

The $^{87}Sr/^{86}Sr$ composition of the leachates from sediment, corresponding to the soluble carbonate fraction (samples-L data, Table 3), is closely consistent with the strontium isotopic composition predicted using biostratigraphy and the strontium seawater curve from Hodell et al. (1991). The Sr-isotope ages of the carbonates define a linear trend and increase with depositional age, from 22.0 to 23.1 Ma, showing slightly older ages, in the error limit, than the biostratigraphic determination (Fig. 5). The carbonate components of the samples do not show strong burial diagenetic chemical overprint. The $^{87}Sr/^{86}Sr$ ratio of the carbonate fraction from the smectite layer is consistent with that of the zeolitic samples, indicating however a minor contribution of a less-radiogenic component in the HAc and HCl-0.1 N leachates compared with the HCl-1 N soluble carbonate fraction.

4.2. The zeolite and clay signatures

The isotopic compositions of the residues (Table 3, Fig. 5) correspond to the authigenic zeolite and to the smectite in the clay layer (Sm1104-R). The Sr-isotopic compositions of the zeolite are not very different from that of the carbonate fractions, showing slightly higher values. The assigned model ages are close to those of the carbonates (Zeolite1114-R) or a little younger (~2 my, Zeolite1094-R, Zeolite1105-R).

Even if a small contribution of unleached carbonate from the bulk rock may not be neglected and would lower the isotopic ratio, it should not affect the significance of the isotopic value of the authigenic fraction. The zeolite signal is higher and thus a significant component of unleached carbonate is unlikely, although contamination by a minor more radiogenic detrital component could be possible. For either case, the data specify that the zeolite genesis uses marine Ca and Sr and is either contemporaneous with or within the early stage of sediment deposition.

The smectite fraction from the thin zeolite-free clay layer (Sm1104-R) shows an unexpected low Sr-isotopic composition. The assigned age is about 50 Ma, which is totally incompatible with the sedimentological constraints. Thus, the contribution of a less-radiogenic component has to be considered, such as a volcanogenic component (most likely reworked aeolian or current-driven input). Such a small less-radiogenic Sr contribution appears to not exceed 15% of the Sr of the mineral, when considering a crustal end-member $^{87}Sr/^{86}Sr$ value of 0.7035 (~value for Caribbean volcanic rocks; *e.g.* Jolly et al., 2001).

The rare earth contents and patterns of the residues (-R) record the same trends (Fig. 6; PAAS-normalized values; Taylor and McLennan, 1985). The zeolitic samples show a negative Ce anomaly (seawater fingerprint) typical of marine sediments and a positive Eu anomaly that reflects

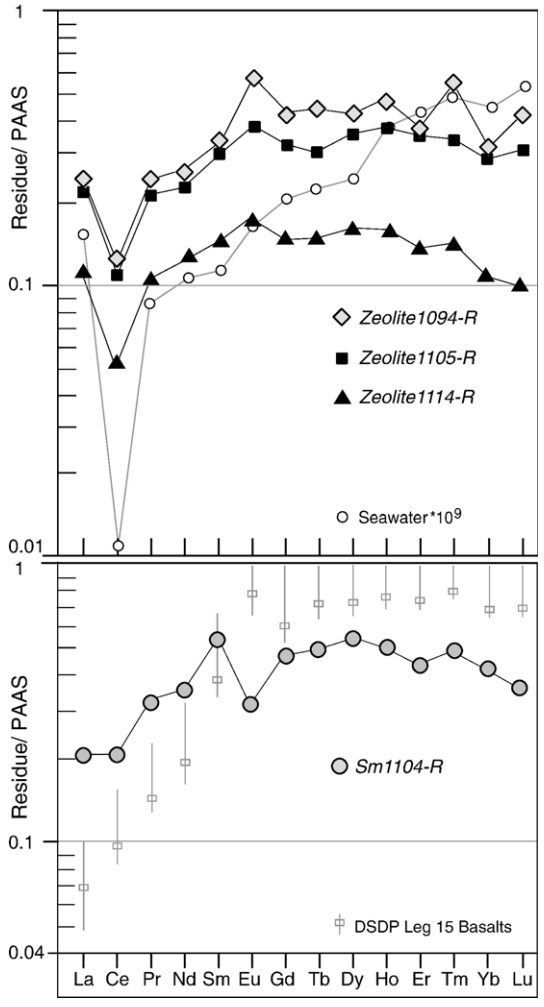

Fig. 6. PAAS-normalized REE patterns of the residues (-R, non-carbonate fractions) of lower Miocene samples from 1090 to 1115 mbsf interval at ODP Site 1007 (PAAS value from Taylor and McLennan, 1985; mean seawater reference from White, 1998; DSDP Leg 15 basalts reference in Sinton et al., 1998).

the selective Eu concentration, which is probably enhanced by recrystallization processes. The Mg smectite (Sm1104-R) has a very different REE pattern, showing depletion in L-REE, slight negative Ce anomaly and negative Eu anomaly. This convex pattern is more similar to that of volcanogenic or basaltic marks on clayey alteration products (Dubinin, 2004; Setti et al., 2004 and references therein).

Thus, from the chemical and isotopic data set it is established that the zeolite formation occurs under marine conditions using marine-derived components. Burial diagenesis proceeding under high W/R ratio is not well evidenced in the stable isotope record ($\delta^{18}O$, $\delta^{13}C$), which preserves the primary composition of the carbonates (Frank and Bernet, 2000; Karpoff et al., 2001; Swart and Eberli, 2005), and did not affect the original Sr-isotope signal. The zeolite precipitation occurs during the early stage of deposition of the carbonate sediments. The remaining question concerns the source of silica involved in this early and rapid formation of clinoptilolite. The sole smectitic thin layer, which does not contain zeolite and overlies the zeolitic sequence, appears to record a different specific source of reactants. The two sedimentary levels exhibit different patterns of evolution in the periplatform Miocene sequences.

5. Modeling of the seawater–sediment alteration: process of clinoptilolite formation

5.1. Saturation index of pore fluids with respect to present-day mineralogy

The interstitial fluids are supersaturated with respect to zeolites, calcite, and quartz, and undersaturated with respect to kaolinite, montmorillonite and opaline silica. Fig. 7 shows the downhole evolution of the logarithm of the saturation index (SI) for secondary minerals observed *in situ*, as well as for common phyllosilicates and a zeolite (K-clinoptilolite) from the KINDIS database (Table 5).

Carbonates are supersaturated throughout the sequence, except for the uppermost fluid at 5.9 mbsf whose chemical composition is close to that of seawater and for lowermost fluids at 986.41 mbsf and 1014.4 mbsf, as a result of the chosen alkalinity value. This is consistent with a carbonate environment. Quartz is supersaturated as well, but opaline silica and kaolinite are undersaturated (Fig. 7A).

The smectites are supersaturated below 500 mbsf, which is consistent with the observations. Zeolite1105 and the K-clinoptilolite are largely supersaturated all along the profile (Fig. 7B). The minerals with a higher Si/Al ratio are favored for supersaturation from the top of the profile, as shown by the high saturation state of K-clinoptilolite (Si/Al=5) compared to the very low saturation state of kaolinite (Si/Al=1). This is also the case for Sm1105, which accumulates the highest Si/Al ratio among the smectites and a high Mg content.

For all minerals, the saturation index changes between 450 mbsf and 550 mbsf. The decrease of the carbonates log(SI) and increase of silicates log(SI) are related to the evolution of the interstitial fluid chemistry to a lower Ca concentration and to a higher Si concentration, respectively (Table 1 and Fig. 8). This limit corresponds to the occurrence of prevalent smectite in the non-carbonate fraction of the sediment, at the upper/middle Miocene boundary. The evolution of the fluid chemistry is consistent with the two main sedimentary domains previously described: (1) the uppermost highly carbonaceous domain controlled by the carbonates (total Ca-molarity and alkalinity varying in opposite way are controlled by the saturation state of calcite), and (2) the lowermost domain containing a larger proportion of phyllosilicates, which combine higher Si and lower Mg fluid concentrations controlled by the smectite precipitation.

At the bottom of the hole, where Sm1105 and Zeolite1105 occur, no pore fluid data are available. As these mineral phases are already supersaturated above 1000 mbsf, their occurrence is consistent with thermodynamics, and they should be the phases controlling the SiO_2 and K concentrations in the interstitial fluids. Moreover no drastic change in the fluid chemistry is needed below 1014 mbsf to allow the prevalence of zeolites and Fe–Mg smectites as non-carbonate minerals.

Thus, the saturation index test confirms the stability of the carbonate environment and of the observed smectites and zeolites. The opaline silica is undersaturated with respect to the interstitial fluids all along the profile and can potentially undergo alteration (*i.e.*, Dixit et al., 2001). At the bottom of the hole where no opaline silica but clinoptilolite is observed, the mineralogical assemblage could be the result of alteration by seawater of a silica-enriched bulk rock. This assumption is tested in the next step of the modeling with three different initial opal contents of the bulk rock.

5.2. Seawater–rock interaction modeling

5.2.1. Estimation of the initial opaline silica content in the smectitic level BR746

The smectitic level BR746 has been considered as being primary sediment, unmodified by further seawater alteration. Thus an opal-A content has to be estimated

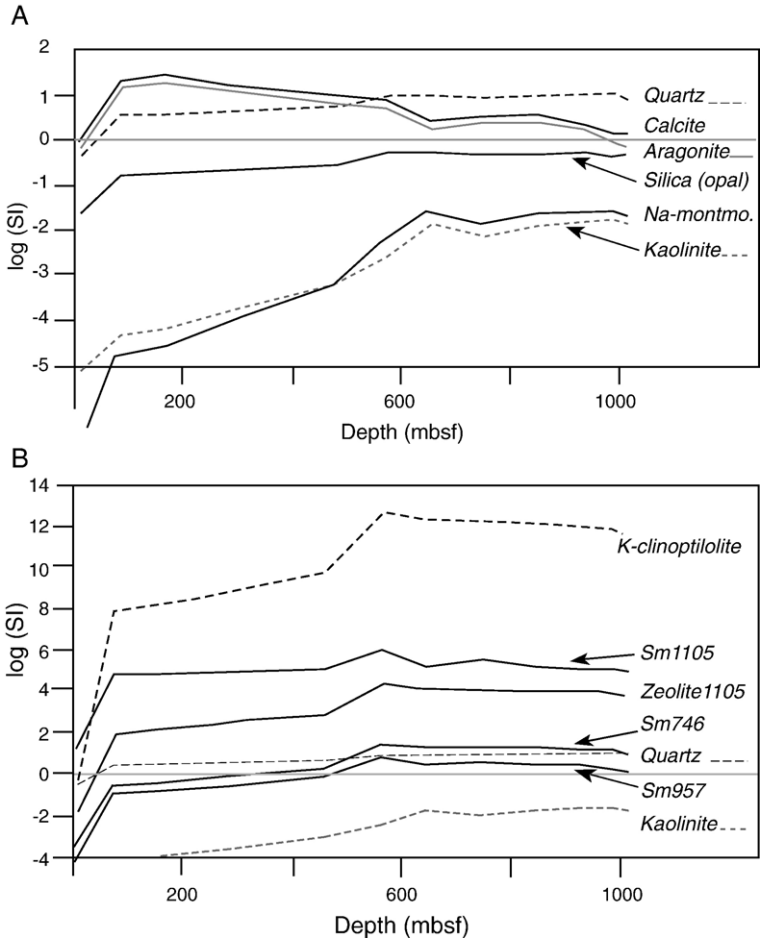

Fig. 7. Evolution along the depth profile of Site 1007 of the interstitial fluids saturation state (log(SI)) (A) towards calcite, aragonite, SiO_2 (opaline silica), Na-montmorillonite and kaolinite, and (B) towards the *in situ* smectites and zeolite, quartz, kaolinite and K-clinoptilolite.

before modeling any process and result of alteration. The potential initial opaline silica content in BR746 was calculated by comparing the chemical composition of the bulk rock with that of its major constituting minerals: calcite, opal and prevalent Sm746 smectite (Tables 2 and 5). A least squares fit, carried out on the major elements, gives the following mineral assemblage made up of calcite (41.9%±2.3), Sm746 (48.6%±5.8), opaline silica (2.3%±3.8) and of minor phases (7.2%± 5.5), as representing best the BR746 chemical composition. The determination coefficient of the fit is 0.995 and the major minerals represent the whole BR746 chemistry to 92.8%. The ~7.2% minor phases account for the initial Na, Fe, K and Ti contents of BR746 and can be explained by accessory K-feldspar or/and illite (<2 wt.%). The calculated mineral assemblage is consistent with the calcite content of 43.2 wt.% calculated by Karpoff et al. (2002), with the assumption that the total Ca belongs to calcite, and with the observations indicating that smectite is the prevalent clay mineral in the bulk rock. Thus, the content of opal in the sediment at 746.1 mbsf (BR746) was estimated at 2.3 wt.%, which corresponds to 4.5 wt.% of the non-carbonate phases.

5.2.2. Test of estimation of the opal content on the zeolite occurrence

Three cases were considered for the seawater alteration modeling. In the first case, the chemical composition of the bulk rock corresponds to that of BR746 without the 2.3 wt.% opaline silica content (BR746-noOP). In the second case, BR746 underwent alteration and, in the third case, 6 wt.% of opaline silica was added to the BR746 chemical composition (BR746-OP). The masses of the secondary minerals produced during alteration are given in Fig. 9. The results of the three calculations are presented as a function of the mass of dissolved calcite in order to focus on the influence of

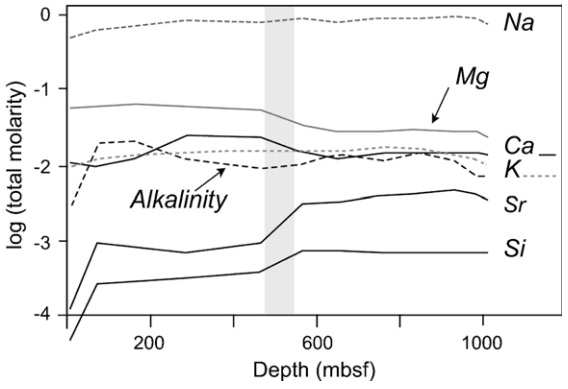

Fig. 8. Evolution of the chemical composition of the interstitial fluids as a function of depth at Site 1007. The grey zone underlines the interval of main change in carbonate's and silicate's saturation states.

opaline silica. Fig. 10 provides, in detail, the evolution of the non-carbonate secondary assemblages.

Among the minerals considered in the modeling, the secondary minerals that precipitate are calcite, smectites, Zeolite1105 and quartz (Fig. 9). The term smectites accounts for the smectites observed *in situ* (Sm746, Sm957 and Sm1105) and for Mg- and Na-montmorillonite end members (Fig. 10). In the three model runs, with or without an opal component, the mass of precipitated calcite equals the mass of dissolved calcite (Fig. 9). This shows that the carbonate content of the sediment is affected neither by seawater alteration nor by opaline silica enrichment in the non-carbonate fraction, which reaches almost 10 wt.% of the bulk rock.

The amount of precipitating smectite is also identical in the three model runs (Fig. 9), but the presence of opaline silica in the bulk rock leads to a slight change in the mineral assemblage, and to the occurrence of zeolite and even quartz (Fig. 10). Sm1105, Sm746 and montmorillonite contribute to the major portion of the non-carbonate phases. Sm746 composes more than 35 wt.% of the secondary assemblage. The concomitant precipitation of Sm1105 and montmorillonite results from the available K and Na supply from seawater for the reaction. The low Si/Al ratio of the montmorillonite balances the high Si/Al ratio of Sm1105. When comparing the alteration of BR746-noOP and of BR746 (Fig. 10A,B), modeling shows that, in the non-carbonate assemblage, more of smectite Sm746 (~50 wt.%) precipitates at the expense of Mg-montmorillonite, since more silica is provided by the bulk rock BR746. Moreover, as alteration proceeds, a Na-rich mineral precipitates as the Na concentration increases in the altering fluid. In the case of the BR746-noOP alteration, Na-montmorillonite precipitates and the bulk rock does not undergo any notable change as the proportion of carbonates and non-carbonate phases remains identical and as the prevalent smectite becomes partly replaced by the same type of smectites (Fig. 10A).

When opaline silica occurs in the sediment, the secondary paragenesis changes with the appearance of zeolite and quartz. In the case of the BR746 alteration (Fig. 10B), Zeolite1105 precipitates and reaches 5 wt.% of the non-carbonate assemblage at the step of 200 g of dissolved calcite (~500 g of dissolved rock or a W/R ratio of about 2). The distribution of the associated smectites slightly changes as the precipitation of smectites with lower Si/Al ratio, such as Sm957, is promoted, and the mass of Sm1105 decreases due to its competition with Zeolite1105 as the K sink.

In the case of BR746-OP alteration (Fig. 10C), Zeolite1105 precipitates earlier and reaches 20 wt.% of the non-carbonate fraction at 50 g of dissolved calcite (~120 g of bulk rock and W/R ~8). Then, it disappears to the advantage of quartz and of Na-montmorillonite, when quartz becomes supersaturated after 100 g of calcite is dissolved. This last mineralogical assemblage shows the constrained possibilities of modeling with respect to natural processes since the KINDIS database is restricted to Zeolite1105 and to K- and Na-end members for clinoptilolites. The model has also to deal with a high silica concentration in the fluid when the W/R ratio (linked to the alteration progress) becomes very low and quartz precipitates. Thus, the observed mineral assemblage with Zeolite1105 could be the signal of an early alteration stage of the sediment, characterized by a high W/R ratio, and corresponds to the early stage of

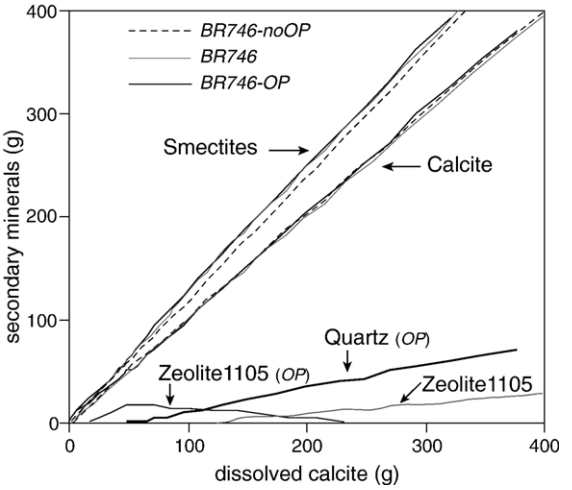

Fig. 9. Comparison of the masses of secondary minerals precipitating during alteration by seawater of the clay level at 746 mbsf (BR746) considering three different opaline silica contents in bulk rock.

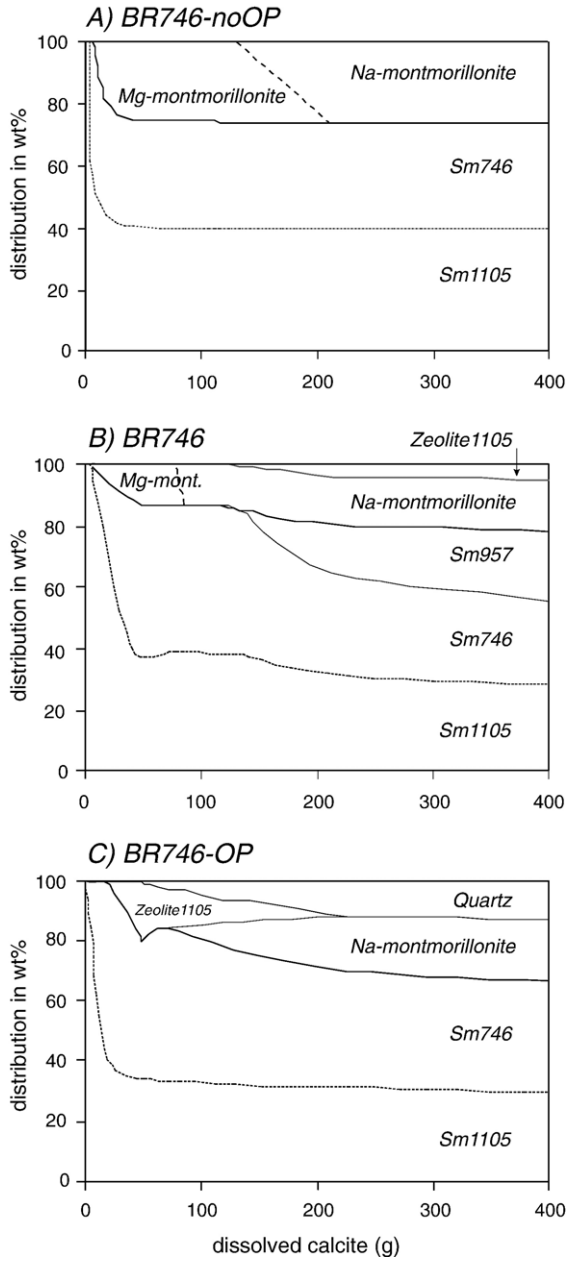

Fig. 10. Distribution of the silicate secondary minerals as a function of the mass of the dissolved calcite, for the seawater alteration of (A) BR746-noOP, (B) BR746, and (C) BR746-OP bulk rocks.

diagenesis with partial compaction and high reactive surfaces. Moreover, the higher the initial opaline silica content is, the earlier is the zeolite occurrence and the higher its proportion in the secondary assemblage.

In summary, the modeling calculations substantiate that the presence of opaline silica is needed in the initial carbonate bulk rock to induce the precipitation of clinoptilolite without any change in the other mineral phases and without any allochthonous volcanogenic contribution. Moreover, a higher opaline silica content induces a larger precipitation of clinoptilolite in the first stages of alteration by seawater. Without any opaline silica in the bulk rock, the equilibrium with seawater is reached because carbonate and smectite remain in the same proportion and composition.

5.3. The zeolite-rich level: estimation of the potential initial opal content and of the present secondary clinoptilolite content

Previous modeling confirmed that the alteration by seawater of opal and smectite of the 746 mbsf unmodified level could lead to a mineral assemblage similar to that observed below at 1105 mbsf, in the zeolite-enriched level. Now, the points to be established are:

- to estimate the initial opaline silica content in the deposit before its alteration, and
- to quantify the actual secondary zeolite proportion in comparison with the proportion predicted by the model.

Both calculations will use the least squares method on the bulk-rock chemical composition of the zeolite-richest sample located at 1104.75 mbsf (BR1105). In the first case, we assume that before alteration, BR1105 was composed of calcite, smectite Sm746, and opaline silica, which are the minerals of the unaltered level (BR746). In the second case, the fit is based on the presently observed mineral assemblage: calcite, Sm1105 and Zeolite1105.

5.3.1. Calculated potential opaline silica content in BR1105

The calculation was carried out on the oxide weight percentages of the major elements (see Table 2), except for Fe_2O_3 wt.% whose high value in BR1105 appears to be mainly due to scarce oxides or pyrite, which will appear in the fit as a part of the minor phases.

As a result, the unaltered BR1105 chemical composition is best represented by the mineral assemblage made up of calcite (64.8%±0.9), Sm746 (13.6%±2.4), opaline silica (8.4%±1.5) and minor phases (5.5%±2.8), with a determination coefficient of 0.999. The result does not account for very minor phases, such as celestine, and possibly variable smectite compositions. Thus, the estimation of the initial opaline silica content ranges from 6.9 to 9.9 wt.% in the bulk rock. For comparison, the opaline silica content of BR746 is only 2.3 wt.%. Therefore an

opal-A content of ~10 wt.% is particularly high in typical carbonate sediments. In the case of Site 1007, it corresponds to about 38 wt.% of the non-carbonate phases.

5.3.2. Clinoptilolite content of the zeolite-rich level BR1105

Considering the minerals observed *in situ*, the best calculated assemblage for the present-day zeolitic level BR1105 is 64.9%±0.8 calcite, 9.0%±5.0 Sm1105, 19.3%±4.5 Zeolite1105 and 6.0%±2.3 accessory minerals, with a determination coefficient of 0.999. The proportion of calcite does not change, compared to that of an unaltered deposit, as calcite is the main sink of calcium and since 20% of Zeolite1105 corresponds only to 0.4 wt.% CaO of the bulk BR1105. In the non-carbonate fraction, the respective proportions of smectite and zeolite are 1/3 and 2/3. The clear prevalence of Zeolite1105 was expected considering both the high initial opaline silica content estimated by the first least squares fit and the modeling results, which predict more zeolite precipitating when more opal-A is dissolved.

5.4. Implication of modeling results on the early diagenesis process

The mass balance calculations on BR1105 sediment show that a non-carbonate primary assemblage consisting of ~8.4% opaline silica and ~13.6% smectite (Sm746) is chemically equivalent to the secondary assemblage comprising ~19.3% clinoptilolite (Zeolite1105) and ~9% smectite (Sm1105). Thus the occurrence of zeolite in the horizon at 1104.75 mbsf indicates seawater alteration of a clay-rich carbonate sediment, together with a significant opal content following the general reaction for silicates:

Biogenic opal + Smectite1 + Seawater
→Clinoptilolite + Smectite2 + Interstitial fluids.

The significant proportion of clinoptilolite estimated in BR1105 sediment results from its high initial opaline silica content. Such a significant amount of opal (~8.4%±1.5 of the bulk rock), consistent with the water–rock reactions modeling, has to be of local biogenic pelagic origin. Wollast (1974), Kastner et al. (1977) and Dixit et al. (2001) have previously observed that the high reactivity of biogenic opal and the competition created by detrital materials, in particular clay minerals, lead to the precipitation of more authigenic Al–Si minerals when opal-A dissolves. Besides, such a large amount of clinoptilolite (2/3 of the non-carbonate fraction) without associated quartz implies an early stage of alteration, characterized by a high W/R ratio, since modeling shows that quartz precipitates when alteration proceeds in a more silica-enriched environment. This could be the case in some deeper sequences, such as the Oligocene/Miocene transition levels, which contain cristobalite, and chert nodules associated with strong cementation features (Eberli et al., 1997). Thus, the observation of authigenic clinoptilolite in the lower Miocene sequence from Site 1007 provides evidence for the initial presence of opaline silica in the carbonate deposit. The biogenic opal signal is fully obliterated once the water–rock reaction occurs. The alteration proceeds during the early stage of deposition and burial diagenesis need not be considered.

6. Discussion

6.1. The in situ water–rock reaction

Sedimentological, hydrochemical and geochemical observations and data indicate that the early diagenetic evolution of the lower Miocene sequence from the GBB is an *in situ* process. The major carbonate phases, showing *in situ* dissolution–precipitation features, do not record a strong burial diagenesis or remobilization signal, as confirmed by their stable isotopic signatures (*e.g.*, Frank and Bernet, 2000; Karpoff et al., 2001; Reuning et al., 2002; Swart and Eberli, 2005) and radiogenic isotopic signatures. The authigenic well-crystallized clinoptilolite occurs in foraminifer tests and matrix, often associated with authigenic celestine.

In oceanic sediments, the precursor for massive zeolite occurrence, together with smectites, is first and commonly considered to be volcaniclastic and basaltic material (*e.g.*, Petzing and Chester, 1979; Riech, 1979; Kastner, 1981; Lee, 1992; Karpoff et al., 1992; Aoki and Kohyama, 1998, and references therein) and, in this case, clinoptilolite is more often ascribed to be a by-product of rhyolitic glass alteration in relation to its higher Si/Al ratio. Some descriptions of authigenic phillipsite or clinoptilolite, as cement in pelagic calcareous oozes from various sites and ages, and related to fluid circulations, have been reported (Bernoulli et al., 1978; Jeans, 1978; McKenzie et al., 1980; Barbieri et al., 1981; Hüggenberg and Füchtbauer, 1988; Wray, 1995; De Ros et al., 1997). However, very few zeolite occurrences in Miocene highly calcareous deposits have been ascribed specifically to increased silica activity in the pore waters, in relation to the dissolution of opal bioclasts (Barbieri et al., 1981; Hüggenberg and Füchtbauer, 1988; De Ros et al., 1997). Observations of direct transformation of siliceous tests into zeolites are scarce and occur in

condensed deep pelagic oozes (Lancelot et al., 1979; Riech, 1979; Karpoff et al., 1981; Bohrmann et al., 1989). A biogenic contribution to Ba-clinoptilolite from a Miocene claystone was reported by Nähr and Bohrmann (1999). It has been established (Nähr et al., 1998) that the formation of clinoptilolite could take place at low temperature (~20 °C) by a direct dissolution–precipitation process.

In summary, all observations and data from the GBB lower Miocene calcareous deposits corroborate that, as suggested earlier by Hay (1977) for pelagic sediments, in the absence of any basaltic or volcaniclastic phases, the genesis of clinoptilolite will be linked to a primary biogenic opal input and its dissolution soon after deposition.

6.2. Process and progress of silicate paragenesis

The marine silicon cycle is intensively studied as it is considered to be a major key to understand the global climate and carbon cycles, since increasing siliceous productivity would be coupled to an enhanced organic carbon burial and subsequent reduced atmospheric pCO_2 (*i.e.*, Dugdale and Wilkerson, 2001; Chikamoto and Yamanaka, 2005; Anderson and Delaney, 2005; and references therein). Oceanic biogenic opal is well-known for its rapid recycling in the water column, and its ability to be very reactive at the water–sediment interface to form authigenic minerals (Wollast, 1974; Kastner et al., 1977; Archer et al., 1993; Nelson et al., 1995; Van Cappellen and Qiu, 1997; Dixit et al., 2001; Greenwood et al., 2001; Chikamoto and Yamanaka, 2005; Fujii and Chai, 2005). The opal preservation–dissolution process in sediments is complex, involving several parameters, such as primary productivity, type and shape of tests, organic matter evolution, calcite and detrital clay fluxes, and kinetics. During burial diagenesis of siliceous pelagic oozes, opal-A undergoes dissolution and re-precipitation stages *via* metastable opal-CT, cristobalite to stable quartz. Detrital material influences the solubility of biogenic silica. The common authigenic minerals ascribed, without quantification, to opal dissolution and its reaction with primary detrital phases are phyllosilicates and more specifically smectites (among others, Johnson, 1976; Kastner, 1981; Mann and Müller, 1985; Karpoff, 1989; Michalopoulos et al., 2000); these smectites are distinct from the detrital ones based on their Si/Al ratio and are in thermodynamic equilibrium with the standard marine environment (T°, pH, contribution of Mg and K from seawater…).

When the biogenic opal input is enhanced in carbonate sediments, then the paragenesis evolves to zeolites. The zeolite formation inhibits cristobalite growth. We have now established that the conversion from authigenic clay to zeolite could occur with 2.3 wt.% of opaline silica in a carbonate deposit. In the GBB periplatform, in the lower Miocene layers from Site 1007, the available biogenic silica is estimated at about 10 wt.% of the whole sediment. With such a high content of reactive silica, the modeling results predict that the amount of clinoptilolite would be significant (~20%) at the beginning of the seawater–rock reaction, and that quartz could precipitate at the expense of clinoptilolite when the alteration proceeds. This later point is consistent with the observation of the lowermost sediments drilled at Site 1007, where small cristobalite or opal-CT lepispheres are observed associated with clinoptilolite crystals and where cristobalite-rich levels (chert nodules) are found at the Oligocene/Miocene boundary layers (Eberli et al., 1997; Karpoff et al., 2002). The sedimentation of reactive opal should also go along with enhanced organic matter input favoring at the same time early diagenesis of the carbonate (dolomite, celestine). Higher preserved Ba content in the sediment also expresses the biogenic opal sign, because barium is commonly considered to be a valuable siliceous productivity proxy (*e.g.*, Kasten et al., 2001; Eagle et al., 2003). As a result, the by-products of biogenic silica dissolution affect the burial evolution and physical properties of the calcareous deposits (*e.g.*, Lancelot, 1973; Hobert and Wetzel, 1989). At GBB Site 1007, the deposits evolved into a highly compacted and lithified level that correlates with the seismic sequence boundary P2 location (23.2 Ma). In the lower Miocene clinoptilolite-rich level (1104.75 mbsf, 21.5–22 Ma) from the GBB, the given water–rock reaction occurred shortly after the deposition, with a high W/R ratio and in a closed system.

6.3. Paleoceanographic implication of authigenic zeolite occurrence

6.3.1. Paleogeographic regional configuration

At time of early Miocene sedimentation, the platform, which already had a flat top and low-angle slope, was established at shallow depths and periplatform oozes dominated in slope and basinal area (Eberli et al., 1997). The Central American seaway was open and the connection across the Caribbean, between intermediate and shallow waters of the Atlantic and Pacific oceans, was well established. Strong regional currents are recorded in marginal formations during early and middle Miocene (Guertin et al., 2000 and references therein). During the early stage of build-up of the platform, after the Oligocene period of tectonic quiescence, several geodynamic events are recorded in

the region: the propagation of the Cayman spreading center, the collision of southern Cuba and the initiation of the collision of Hispaniola with the Bahamas (*e.g.*, Meschede and Frisch, 1998). These events do not seem to have deeply modified or controlled the sedimentary architecture. In the central Caribbean Sea, explosive volcanic events are documented in cored sections by ash layers. Major volcanism episodes are reported in late Oligocene and continued in late early Miocene through middle Miocene (Sigurdsson et al., 2000).

In the GBB lower Miocene sediments, the characteristics of peculiar thin, smectite-rich, zeolite-free layers (*ex. at 1104.54 mbsf*) interbedded in the wackestone sequence appear to be likely linked to a contribution, wind or current-driven, of an ash-derived alteration product related to the sporadic volcanic activity of the Caribbean region. Ash layers or volcaniclastic detritus are not observed in the Miocene sedimentary pile, thus the chemical volcanic trace only recorded in clay layers seems provided by small amounts of imported secondary by-products. Nevertheless and evidently, the significance of the major change in the pelagic production at Site 1007, with high silica incursion now expressed by the authigenic zeolite–smectite assemblage and its chemical specificities, has to be evaluated both at the regional and global scales.

6.3.2. Oceanographic and environmental changes at the Oligocene–early Miocene transition

The Oligocene/Miocene boundary (23.8 Ma *in* Eberli et al., 1997; 22.9 Ma *in* Shackleton et al., 2000) is marked by significant paleoceanographic variation and crisis linked to the onset of the Antarctic glaciation with the extension of the East Antarctic ice sheet that oscillates during the early Miocene times, and the establishment of the Antarctic Circumpolar Current (ACC). Before the mid-Miocene global cooling, during the earliest Miocene the main transient Antarctic glaciation episodes, inferred from oxygen isotope data, are reported as Mi-1 and Mi-1a events (Miller et al., 1991; Paul et al., 2000; Zachos et al., 2001a,b; Naish et al., 2001). The global glacial Mi-1 event also coincides with well-correlated orbital obliquity and eccentricity cycles (Zachos et al., 2001a). The Mi-1 and Mi-1a oxygen isotope excursion events are commonly assigned age of 23.5 Ma and 21.2 Ma, respectively (Miller et al., 1991; Wright and Miller, 1992), and were recently calibrated as 22.95 Ma and 21.1 Ma in equatorial Atlantic pelagic sections (Paul et al., 2000). The related decrease of deep-water temperature is generally estimated to be about ~3 °C (Zachos et al., 1997; Paul et al., 2000). On another hand, for more local scale issue, recent studies relate the disappearance of corals species in the Caribbean Sea at the Oligocene/Miocene transition to the sudden intrusion of Pacific waters, enhancing further regional pelagic productivity (von der Heydt and Djikstra, 2005; Mutti et al., 2005).

Thus, in the GBB earliest Miocene deposits, the zeolite authigenesis that traces an enhanced biogenic silica contribution to the carbonate sedimentation appears to be coeval with the globally recognized Mi-1 and Mi-1a events. But changes in surface water temperature in such a tropical area, when related to oxygen isotope events, are expected to be minor. It is noticed that the environmental changes at Site 1007 (temperature, nutrients…) were sufficient to induce a high silica productivity and sedimentation. This enhanced productivity is also recorded by an increased organic carbon flux (Kramer et al., 2000) and by trace elements concentration (*e.g.*, Ba). The type of biogenic production (*i.e.*, diatoms, radiolarians…) can no longer be identified as this biogenic silica input that was rapidly altered to an authigenic clinoptilolite–smectite assemblage by an early diagenetic reaction, which is the sedimentary record of this paleoceanographical event.

In turn, such a sensitive and responsive mineralogical expression of a paleoceanographical change should not be restricted to only the early Miocene events, but should also be a potential cyclicity trace. As a matter of fact, at Site 1003 closer to the banktop, a mid-Miocene sequence (~12.7–13 Ma) contained small-scale depositional cycles which is the first observation of coeval occurrences of authigenic Mg smectite and scarce clinoptilolite closely linked to the cyclic alternations of light-grey well-cemented and dark-grey uncemented layers (Karpoff et al., 2003). Further age calibrations of these occurrences and their links with other productivity proxies are required to specify the paleoceanographical and/or orbital record in this mid-Miocene sequence. Moreover, this mineralogical proxy should be more efficient for monotonous calcareous sequences lacking in volcaniclastic matter, than in polygenetic deep-sea pelagic deposits.

7. Conclusion

In the Great Bahama Bank periplatform during the early Miocene period of carbonate sedimentation, diagenetic seawater–sediment interactions occurred very soon after deposition and ended to form an authigenic silicate assemblage comprising Mg smectite and clinoptilolite. The massive formation of zeolite, not often observed in shallow-water carbonates represents up to 20% of the bulk rock, and is interpreted to be of penecontemporaneous marine origin based on the Sr-isotopic signature and the

modeling of the water–rock interaction. The reaction between primary opaline silica, equivalent to an input of about 10% of biogenic opal-A to the deposit, and primary silicates involves the full loss of biogenic tests and the neoformation of the new paragenesis. The observed diagenesis requires a significant input of opal which is probably related to major oceanographic changes in pelagic production, most likely linked to the global Mi-1 and Mi-1a glacial events (23.5–21.2 Ma). Thus, the presence of clinoptilolite can be a very precise marker for enhanced productivity in carbonate sequences free of volcaniclastic supply, and the authigenic silicate paragenesis can be used as a proxy for marine climatic change record in sensitive zones, such as the marginal seas.

Acknowledgements

This paper is dedicated to the memory of Sir N. Shackleton. Our sincere thanks go to Judith A. McKenzie for her interest and comments to improve the manuscript. We thank John J.G. Reijmer (CEREGE, Aix) and Stefano Bernasconi (ETH-Zurich) for their constant support to our studies. ODP Leg 166 co-chiefs and scientific team are thanked for providing the opportunity of sampling during the membership of Pascale Déjardin to the cruise. The authors are grateful to P. Karcher for valuable technical support on SEM, and to J.J. Frey and T. Perrone for their help in the isotope laboratory. We appreciate the very helpful comments and suggestions from Linda Anderson, an anonymous reviewer, and Lynn Walter.

This work is the contribution 2007.401-UMR7517 of CGS-EOST.

References

Anderson, L.D., Delaney, M.L., 2005. Use of multiproxy records on the Agulhas Ridge, Southern Ocean (Ocean Drilling Project Leg 177, Site 1090) to investigate sub-Antarctic hydrography from the Oligocene to the early Miocene. Paleoceanography 20 (3), 1–16. doi:10.1029/2004PA001082 PA3011.

Anselmetti, F.S., Eberli, G.P., Ding, Z.-D., 2000. From the Great Bahama Bank into the straits of Florida: a margin architecture controlled by sea-level fluctuations and ocean current. Bull. Geol. Soc. Am. 112 (6), 829–844.

Aoki, S., Kohyama, N., 1998. Cenozoic sedimentation and clay mineralogy in the northern part of the Magellan Trough, Central Pacific Basin. Mar. Geol. 148, 21–37.

Archer, D., Lyle, M., Rodgers, K., Froelich, P., 1993. What controls opal preservation in tropical deep-sea sediments? Paleoceanography 8, 7–21.

Banner, J.L., 1995. Application of the trace element and isotope geochemistry of strontium to studies of carbonate diagenesis. Sedimentology 42, 805–824.

Barbieri, M., Bellanca, A., Neri, R., 1981. Origin of zeolites associated with montmorillonite and silica phases in Miocene deposits of Sicily. Acta Mineral.-Petrogr. 25, 41–55.

Bernoulli, D., Garrison, R.E., Mélières, F., 1978. Phillipsite cementation in a foraminiferal sandstone at Hole 373A and "the case of the violated foram". In: Hsü, K.J., Montadert, L., et al. (Eds.), Init. Repts. DSDP 42, Washington (U.S. Govt Printing Office), pp. 478–482.

Betzler, C., Reijmer, J.J.G., Bernet, K., Eberli, G.P., Anselmetti, F.S., 1999. Sedimentary patterns and geometries of the Bahamian outer carbonate ramp (Miocene–Lower Pliocene, Great Bahama Bank). Sedimentology 46 (6), 1127–1143.

Betzler, C., Pfeiffer, M., Saxena, S., 2000. Carbonate shedding and sedimentary cyclicities of a distally steepened carbonate ramp (Miocene, Great Bahama Bank). Int. J. Earth Sci. 89, 140–153.

Bohrmann, G., Stein, R., Faugères, J.-C., 1989. Authigenic zeolites and their relation to silica diagenesis in ODP Site 661 sediments (Leg 108, Eastern Equatorial Atlantic). Geol. Rundsch. 78, 779–792.

Camoin, G.F., Dullo, W.-Ch., 1999. Paleoceanography of reefs and carbonate platforms: Miocene to Modern. Abstracts Book, Pub. Ass. Fr. Sedim., Paris. 231 pp.

Caspard, F., Rudkiewicz, J.L., Eberli, G.P., Brosse, E., Renard, M., 2004. Massive dolomitization of a Messinian reef in the Great Bahama Bank: a numerical modelling evaluation of Kohout geothermal convection. Geofluids 4, 40–60.

Chermak, J.A., Rimstidt, J.D., 1989. Estimating the thermodynamic properties (ΔG_f^0 and ΔH_f^0) of silicate minerals at 298 K from the sum of polyhedral contributions. Am. Mineral. 74, 1023–1031.

Chikamoto, M.O., Yamanaka, Y., 2005. Sedimentary responses to an abrupt change of biogenic silica flux by a sediment model for long timescale simulations. J. Oceanography 61, 733–746.

De Carlo, E.H., Kramer, P.A., 2000. Minor and trace elements in interstitial waters of the Great Bahama Bank: results from ODP Leg 166. In: Swart, P.K., Eberli, G.P., Malone, M.J., Sarg, J.F., Proc. ODP, Sci. Results 166, College Station TX (Ocean Drilling Program), pp. 99–111.

DePaolo, D.J., Ingram, B.L., 1985. High resolution stratigraphy with strontium isotopes. Science 277, 938–941.

De Ros, L.F., Morad, S., Al-Aasm, I.S., 1997. Diagenesis of siliciclastic and volcaniclastic sediments in the Cretaceous and Miocene sequences of the NW African Margin (DSDP Leg 47A, Site 397). Sediment. Geol. 112, 137–156.

Dixit, S., Van Cappellen, P., van Bennekom, A.J., 2001. Processes controlling solubility of biogenic silica and pore water build-up of silicic acid in marine sediments. Mar. Chem. 73, 333–352.

Dubinin, A.V., 2004. Geochemistry of rare earth elements in the ocean. Lithol. Miner. Resour. 39 (4), 339–358.

Dugdale, R.C., Wilkerson, F.P., 2001. Source and fates of silicon in the ocean: the role of diatoms in the climate and glacial cycles. In: Gili, J.M., Pretus, J.L., Packard, T.T. (Eds.), A Marine Science Odyssey into the 21st Century. Sci. Mar., vol. 65, 2, pp. 141–152.

Eagle, M., Paytan, A., Arrigo, K.R., van Dijken, G., Murray, R.W., 2003. A comparison between excess barium and barite as indicators of carbon export. Paleoceanography 18 (1), 1021. doi:10.1029/2002PA000793.

Eberli, G.P., 1991. Growth and demise of isolated carbonate platforms: Bahamian controversies. In: Müller, D.V., McKenzie, J.A., Weissert, H. (Eds.), Controversies in Modern Geology. Academic Press, London, pp. 231–248.

Eberli, G.P., Swart, P.K., Malone, M.J., et al., 1997. Proc. ODP, Init. Repts. 166, College Station, TX (Ocean Drilling Program).

Elderfield, H., Swart, P.K., McKenzie, J.A., Williams, A., 1993. The strontium isotopic composition of pore waters from Leg 133: northeast Australian margin. In: McKenzie, J.A., Davies, P.J., Palmer-Julson, A. et al., Proc. ODP, Sci. Results 133, College Station, TX (Ocean Drilling Program), 473–480.

Frank, T.D., Bernet, K., 2000. Isotopic signature of burial diagenesis and primary lithological contrasts in periplatform carbonates (Miocene, Great Bahama Bank). Sedimentology 47 (6), 1119–1134.

Fujii, M., Chai, F., 2005. Effects of biogenic silica dissolution on silicon cycling and export. Geophys. Res. Lett. 32, L05617. doi:10.1029/2004GL022054.

Greenwood, J.E., Truesdale, V.W., Rendell, A.R., 2001. Biogenic silica dissolution in seawater — in vitro chemical kinetics. Prog. Oceanogr. 48, 1–23.

Guertin, L.A., Missimer, T.M., McNeill, D.F., 2000. Hiatal duration of correlative sequence boundaries from Oligocene–Pliocene mixed carbonate/siliciclastic sediments of the south Florida Platform. Sediment. Geol. 134, 1–26.

Haq, B.U., Hardenhol, J., Vail, P.R., 1987. Chronology of fluctuating sea level since the Triassic. Science 235, 1156–1167.

Hay, R.L., 1977. Geology of zeolites in sedimentary rocks. In: Mumpton, F.A. (Ed.), Mineralogy and Geology of Natural Zeolites. Miner. Soc. Amer. Short Courses Notes, vol. 4, pp. 53–64.

Helgeson, H.C., Delany, J.M., Nesbitt, H.W., Bird, D.K., 1978. Summary and critique of the thermodynamic properties of rock-forming minerals. Am. J. Sci. 278A, 1–229.

Henderson, G.M., Slowey, N.C., Haddad, G.A., 1999. Fluid flow through carbonate platforms: constraints from $^{234}U/^{238}U$ and Cl− in Bahamas pore-waters. Earth Planet. Sci. Lett. 169, 99–111.

Hobert, L., Wetzel, A., 1989. On the relationship between silica and carbonate diagenesis in deep-sea sediments. Geol. Rundsch. 78, 765–778.

Hodell, D.A., Mueller, P.A., Garrido, J.R., 1991. Variations in the strontium isotopic composition of seawater during the Neogene. Geology 19, 24–27.

Hüggenberg, H., Füchtbauer, H., 1988. Clay mineral and their diagenesis in carbonate-rich sediments (Leg 101, Sites 626 and 627). In: Austin, J.A., Schlager, W. et al., Proc. ODP, Sci. Results 101, College Station, TX (Ocean Drilling Program), 171–177.

Jeans, C.V., 1978. Silicifications and associated clay assemblages in the Cretaceous marine sediments of southern England. Clay Miner. 13, 101–126.

John, C.M., Mutti, M., Adatte, Th., 2003. Mixed carbonate-siliciclastic record on the North African margin (Malta) — coupling of weathering processes and mid Miocene climate. Geol. Soc. Amer. Bull. 115 (2), 217–229.

Johnson, T.C., 1976. Biogenic opal preservation in pelagic sediments of a small area in the eastern tropical Pacific. Geol. Soc. Amer. Bull. 87, 1273–1282.

Jolly, W.T., Lidiak, E.G., Dickin, A.P., Wu, T.W., 2001. Secular geochemistry of central Puerto Rican island arc lavas: constraints on Mesozoic tectonism in the Greater Antilles. J. Petrol. 42, 2197–2214.

Karpoff, A.M., 1989. Les séries pélagiques condensées du Cénozoïque des océans Pacifique et Atlantique: témoins des grandes crises géodynamiques. Doc. ès Sci. Thesis, ULP Strasbourg, France, 255 pp.

Karpoff, A.M., Hoffert, M., Clauer, N., 1981. Sedimentary sequences at Site 464: silicification processes and transition between siliceous biogenic oozes and Brown Clays. In: Thiede, J., Vallier, T.L. et al., Init. Repts. DSDP 62, Washington (U.S. Govt Printing Office), pp. 759–771.

Karpoff, A.M., France-Lanord, C., Lothe, F., Karcher, P., 1992. Miocene tuff from Mariana Basin, Leg 129, Site 802: a first deep-sea occurrence of thaumasite. In: Larson, R.L., Lancelot, Y. et al., Proc. ODP, Sci. Results 129, College Station, TX (Ocean Drilling Program), pp. 119–135.

Karpoff, A.M., Bernasconi, S., Destrigneville, C., Stille, P., 2001. Diagenetic zeolite and clay minerals in Miocene Great Bahama Bank carbonate sediments (ODP Leg 166, Site 1007). In: Cidu, R. (Ed.), Water–Rock Interaction—WRI10 Proceedings Balkema Publ., pp. 623–626.

Karpoff, A.M., Destrigneville, C., Bartier, D., Déjardin, P., 2002. Phyllosilicates and zeolite assemblages in the carbonate periplatform of the Great Bahama Bank: origin and relation to diagenetic processes (ODP Leg 166, Sites 1006 and 1007). Mar. Geol. 185, 55–74.

Karpoff, A.M., Destrigneville, C., Stille, P., Reijmer, J.J.G., 2003. Record of paleoclimatic changes and paleoproductivity events from clay minerals and zeolite parageneses in Great Bahama Bank carbonate sediments (ODP Leg 166). Euroclay 2003, 10th Conf. EGCA, Univ. di Modena, Italy (Ed.), pp. 147–148.

Kasten, S., Haese, R.R., Zabel, M., Ruhlemann, C., Schulz, H.D., 2001. Barium peaks at glacial terminations in sediments of the equatorial Atlantic Ocean — relicts of deglacial productivity pulses? Chem. Geol. 175, 635–651.

Kastner, M., 1981. Authigenic silicates in deep sea sediments: formation and diagenesis. In: Emiliani, C. (Ed.), The Oceanic Lithosphere. The Sea, 7, Wiley Interscience Pub. John Wiley & Sons, New York, pp. 915–980.

Kastner, M., Keene, J.B., Gieskes, J.M., 1977. Diagenesis of siliceous oozes — I. Chemical control on the rate of opal-A to opal-CT transformation, an experimental study. Geochim. Cosmochim. Acta 41, 1041–1059.

Kramer, P.A., Swart, P.K., De Carlo, E.H., Schovsbo, N.H., 2000. Overview of interstitial fluid and sediment geochemistry, Sites 1003–1007 (Bahamas transect). In: Swart, P.K., Eberli, G.P., Malone, M.J., Sarg, J.F., Proc. ODP, Sci. Results 166, College Station TX (Ocean Drilling Program), pp. 179–195.

Lancelot, Y., 1973. Chert and silica diagenesis in sediments from the central Pacific, Leg 17, Deep Sea Drilling Project. In: Winterer, E.L., Ewing, J.I. et al., Init. Repts. DSDP 17, Washington (U.S. Govt. Printing Office), pp. 577–605.

Lancelot, Y., Sliter, W.V., Westberg, J., 1979. Evidence of direct transformation of radiolarians into zeolites in mid-Cretaceous deep sea clays. Geol. Soc. Amer. Ann. Meeting Abstract, p. 492.

Lee, Y.I., 1992. Diagenesis of deep-sea volcaniclastic sandstones. In: Wolf, K.H., Chilingarian, G.V. (Eds.), Diagenesis III. Developments in Sedimentology, vol. 47, pp. 253–290.

Madé, B., Clément, A., Fritz, B., 1990. Modélisation cinétique et thermodynamique de l'altération: le modèle géochimique KINDIS. C. R. Acad. Sci., Paris 308, 647–654.

Malone, M.J., Slowey, N.C., Henderson, G.M., 2001. Early diagenesis of shallow-water periplatform carbonate sediments, leeward margin, Great Bahama Bank (Ocean Drilling Program Leg 166). Geol. Soc. Amer. Bull. 113 (7), 881–894. doi:10.1130/0016-7606(2001)113<0881:EDOSWP>2.0.CO;2.

Mann, U., Müller, G., 1985. Early diagenesis of biogenic siliceous constituents in silty clays and claystones, Japan Trench. Neues Jahrb. Mineral. Abh. 153, 33–57.

McKenzie, J.A., Bernoulli, D., Schlanger, S.D., 1980. Shallow-water carbonate sediments from Emperor Seamounts: their diagenesis and paleoceanographic significance. In: Jackson, E.D., Koizumi, I. et al., Init. Repts. DSDP 55, Washington (U.S. Govt Printing Office), pp. 415–455.

McKenzie, J.A., Davies, P.J., Palmer-Julson, A., et al., 1993. Proc. ODP, Sci. Results 133, College Station TX (Ocean Drilling Program).

Melim, L.A., Westphal, H., Swart, P.K., Eberli, G.P., Munnecke, A., 2002. Questioning carbonate diagenetic paradigms: evidence from the Neogene of the Bahamas. Mar. Geol. 185, 27–53.

Meschede, M., Frisch, W., 1998. A plate-tectonic model for the Mesozoic and Early Cenozoic history of the Caribbean plate. Tectonophysics (Amst.) 296, 269–291.

Michalopoulos, P., Aller, R.C., Reeder, R.J., 2000. Conversion of diatoms to clays during early diagenesis in tropical, continental shelf muds. Geology 28, 1095–1098.

Miller, K.G., Wright, J.D., Fairbanks, R.G., 1991. Unlocking the ice house: Oligocene–Miocene oxygen isotopes, eustasy, and margin erosion. J. Geophys. Res. 96, 6829–6848.

Mutti, M., Bernoulli, D., Stille, P., 1997. Temperate carbonate platform drowning linked to Miocene oceanographic events: Maiella platform margin, Italy. Terra Nova 9, 122–125.

Mutti, M., Droxler, A.W., Cunningham, A.D., 2005. Evolution of the Northern Nicaragua Rise during the Oligocene–Miocene: drowning by environmental factors. Sediment. Geol. 175, 237–258.

Nagihara, S., Wang, K., 2000. Geothermal regime of the Western margin of the Great Bahama Bank. In: Swart, P.K., Eberli, G.P., Malone, M.J., Sarg, J.F., Proc. ODP, Sci. Results 166, College Station TX (Ocean Drilling Program), pp. 113–120.

Nähr, T., Bohrmann, G., 1999. Barium-rich authigenic clinoptilolite in sediments from the Japan Sea — a sink for dissolved barium? Chem. Geol. 158, 227–244.

Nähr, T., Botz, R., Bohrmann, G., Schmidt, M., 1998. Oxygen isotopic composition of low-temperature authigenic clinoptilolite. Earth Planet. Sci. Lett. 160 (3–4), 369–381.

Naish, T.R., Woolfe, K.J., Barret, P.J., et al., 2001. Orbitally induced oscillations in the East Antarctic ice sheet at the Oligocene/Miocene boundary. Nature 413, 719–723.

Nelson, D.M., Tréguer, P., Brzezinski, M.A., Leynaert, A., Quéguiner, B., 1995. Production and dissolution of biogenic silica in the ocean: revised global estimates, comparison with regional data and relationship to biogenic sedimentation. Glob. Biogeochem. Cycles 9 (3), 359–372.

Paul, H.A., Zachos, J.C., Flower, B.J., Tripati, A., 2000. Orbitally induced climate and geochemical variability across the Oligocene/Miocene boundary. Paleoceanography 15 (5), 471–485.

Petzing, J., Chester, R., 1979. Authigenic marine zeolites and their relationship to global volcanism. Mar. Geol. 29, 253–271.

Reijmer, J.J.G., Betzler, C., Kroon, D., Tiedemann, R., Eberli, G.P., 2002. Bahamian carbonate platform development in response to sea-level changes and the closure of the Isthmus of Panama. Int. J. Earth Sci. 91 (3), 482–489.

Reuning, L., Reijmer, J.J.G., Betzler, C., 2002. Sedimentation cycles and their diagenesis on the slope of a Miocene carbonate ramp (Bahamas, ODP Leg 166). Mar. Geol. 185, 121–142.

Riech, V., 1979. Diagenesis of silica, zeolites and phyllosilicates at Sites 397 and 398. In: von Rad, U., Ryan, W.B.F. et al., Init. Repts. DSDP 47, Washington (U.S. Govt Printing Office), pp. 741–759.

Roof, S.R., Mullins, H.T., Gartner, S., Huang, T.C., Joyce, E., Prutzman, J., Tjalsma, L., 1991. Climatic forcing of cyclic carbonate sedimentation during the 5.4 million years along the West Florida continental margin. J. Sediment. Petrol. 61, 1070–1088.

Samuel, J., Rouault, R., Besnus, Y., 1985. Analyse multiélémentaire standardisée des matériaux géologiques en spectrométrie d'émission par plasma à couplage inductif. Analusis 13, 312–317.

Setti, M., Marinoni, L., López-Galindo, A., 2004. Mineralogical and geochemical characteristics (major, minor, trace elements and REE) of detrital and authigenic clay minerals in a Cenozoic sequence from Ross Sea, Antarctica. Clay Miner. 39, 405–421.

Shackleton, N.J., Hall, M.A., Raffi, I., Tauxe, L., Zachos, J., 2000. Astronomical calibration age for the Oligocene–Miocene boundary. Geology 28, 447–450.

Shipboard Scientific Party, 1997. Explanatory notes. In: Eberli, G.P., Swart, P.K., Malone, M.J. et al., Proc. ODP, Init. Repts. 166, College Station, TX (Ocean Drilling Program), pp. 43–65.

Sigurdsson, H., Kelley, S., Leckie, R.M., Carey, S., Bralower, T., King, J., 2000. History of circum-caribbean explosive volcanism: $^{40}Ar/^{39}Ar$ dating of tephra layers. In: Leckie, R.M., Sigurdsson, H., Acton, G.D., Draper, G., Proc. ODP, Sci. Results 165, College Station, TX (Ocean Drilling Program), pp. 299–314.

Sinton, C.W., Duncan, R.A., Storey, M., Lewis, J., Estrada, J.J., 1998. An oceanic flood basalt province within the Caribbean plate. Earth Planet. Sci. Lett. 155, 221–235.

Steinmann, M., Stille, P., 1997. Rare earth element behaviour and Pb, Sr, Nd isotope systematics in a heavy metal contaminated soil. Appl. Geochem. 12, 607–623.

Swart, P., 2000. The oxygen isotopic composition of interstitial waters: evidence for fluid flow and recrystallization in the margin of Great Bahama Bank. In: Swart, P., Eberli, G.P., Malone, M.J., Sarg, J.F., Proc. ODP, Sci. Results 166, College Station, TX (Ocean Drilling Program), pp. 91–98.

Swart, P., Eberli, G.P., 2005. The nature of the $\delta^{13}C$ of periplatform sediments: implications for stratigraphy and the global carbon cycle. Sediment. Geol. 175, 115–129.

Swart, P., Eberli, G.P., Malone, M.J., Sarg, J.F., 2000. Proc. ODP, Sci. Results 166, College Station, TX (Ocean Drilling Program).

Taylor, S.R., McLennan, S.M., 1985. The Continental Crust: Its Composition and Evolution. Blackwell, Oxford.

Van Cappellen, P., 1996. Reactive surface area control of the dissolution kinetics of biogenic silica in deep-sea sediments. Chem. Geol. 132, 125–130.

Van Cappellen, P., Qiu, L., 1997. Biogenic silica dissolution in sediments of the Southern Ocean. II. Kinetics. Deep-Sea Res., Part 2, Top. Stud. Oceanogr. 44, 1129–1149.

von der Heydt, A., Djikstra, H.A., 2005. Flow reorganization in the Panama Seaway: a cause for the demise of Miocene corals. Geophys. Res. Lett. 32, L02609. doi:10.1029/2004GL020990.

White, W.M., 1998. Geochemistry. Chapter 15—the Oceans as a Chemical System. Cornell University. An on-line texbook at: http://www.geo.cornell.edu/geology/classes/geo455/Chapters.html.

Winterer, E.L., Sager, W.W., Firth, J.V., Sinton, J.M., 1995. Proc. ODP, Sci. Results 143, College Station, TX (Ocean Drilling Program).

Wollast, R., 1974. The silica problem. In: Goldberg, E.D. (Ed.), Marine Chemistry. The Sea, vol. 5. Wiley-Interscience Pub., pp. 359–392.

Wray, D.S., 1995. Origin of clay-rich beds in Turonian chalks from Lower Saxony, Germany — a rare earth element study. Chem. Geol. 119, 161–173.

Wright, J.D., Miller, K.G., 1992. Miocene stable isotope stratigraphy, Site 747, Kerguelen Plateau. In: Wise, S.W., Schlich, R., Proc. ODP, Sci. Results 120, College Station, TX (Ocean Drilling Program., pp. 855–866.

Zachos, J.C., Flower, B.P., Paul, H.A., 1997. Orbitally paced climate oscillations across the Oligocene/Miocene boundary. Nature 388, 567–570.

Zachos, J.C., Shackleton, N.J., Revenaugh, J.S., Pälike, H., Flower, B., 2001a. Climate response to orbital forcing across the Oligocene–Miocene boundary. Science 292, 274–278.

Zachos, J., Pagani, M., Sloan, L., Thomas, E., Billups, K., 2001b. Trends, rhythms, and aberrations in global climate 65 Ma to Present. Science 292, 686–693.